

MASS ACTION KINETICS OF VIRUS-CELL AGGREGATION AND FUSION

JOE BENTZ,* SHLOMO NIR,[†] AND DAVID G. COVELL[‡]

**Departments of Pharmacy and Pharmaceutical Chemistry, School of Pharmacy, University of California, San Francisco, California 94143; [†]Seagram Centre for Soil and Water Science, Faculty of Agriculture, Hebrew University, Rehovot 76-100, Israel; and [‡]Laboratory of Mathematical Biology, National Cancer Institute, Bethesda, Maryland 20892*

ABSTRACT A simple approximate solution for the mass action kinetics of small particles (viruses or vesicles) binding to large particles (cells) and their subsequent fusion has been derived. The solution is evaluated in terms of the measurable fluorescence changes expected when the virus or vesicles are labeled with fluorescent probes, which are diluted into the cellular membrane by fusion. Comparison with numerical integrations shows that the approximate solution is extremely accurate. Analytic simplifications for a variety of special cases of this general problem are also shown.

INTRODUCTION

The adhesion of vesicles and virions to cells, and the subsequent fusion between the membranes, has been studied from many perspectives (White et al., 1983; Redmond et al., 1984; Citovsky et al., 1985; Doxsey et al., 1985; van Meer et al., 1985; Stegmann et al., 1985, 1986, 1987a-c; Hoekstra et al., 1985; Hoekstra and Klappe, 1986; Richman et al., 1986). Much of the recent work has involved kinetic analyses, aimed at obtaining the rate constants for the aggregation and/or fusion steps (Kuroda et al., 1985; Nir et al., 1986a-c; Tsao and Huang, 1986; Blumenthal et al., 1987). Quantitative studies, such as these, are necessary to elucidate the molecular mechanisms of close apposition between membranes and their subsequent fusion (Blumenthal, 1987; Bentz and Ellens, 1988; Bentz et al., 1988).

Standard kinetic equations describing the vesicle-cell aggregation and fusion reactions are typically difficult to solve, often involving 10^4 coupled nonlinear equations. To facilitate the usage of the kinetic analysis, we have developed a simple solution for one class of these problems, which includes virus aggregation and fusion with cells, as well as particle-macrophage interactions. Specifically, we have treated the problem of small particles binding and fusing with a larger particle. Our first focus is the case where the binding/fusion sites on the larger particle's surface are identical and independent of the neighboring sites. In this limit, the kinetics are comparable to the situation where all sites are homogeneously distributed within the reaction volume. By inclusion of the fusion step, this work extends the treatments given by Yassky (1962), Gani (1965, 1967), Perelson (1985), and Brendel and

Perelson (1987) for the aggregation of small and large particles. In addition, we have coupled these kinetics to specific fluorometric assays commonly in use for virus-cell fusion and developed a very simple formula for the time course of fluorescence intensity changes.

We have also considered the case where the binding sites are not independent, i.e., virus bound to a site shields an adjacent binding site. This reduces the higher order aggregation rate constants. The effect of this shielding can be measured and minimized simply by increasing the concentration of cells, i.e., increasing the number of vacant binding sites so that near neighbor interactions become unlikely. On the other hand, when fusion is rate limited by irreversible aggregation, we have found nearly analytical solutions for fluorescence intensity and the concentration of each of the fusion products. These solutions are given in terms of an effective time parameter, which is evaluated by a single-numerical integration. This case subsumes that of irreversible binding of small to large particles.

Several approximate solutions are presented for limiting cases and their accuracy is estimated from numerical calculations. The reliability of the approximate solutions implies that one may use the homogeneous approximation whenever the binding sites are independent. Furthermore, although it is known that virus-cell adhesion can be reversible (Hoekstra and Klappe, 1986), our results indicate that this reversibility can be measured reliably only by preincubation of the system under nonfusogenic conditions (e.g., low temperature) followed by a jump to the fusogenic condition (e.g., 37°C). The simplest equations for analyzing fusion after preincubation are described.

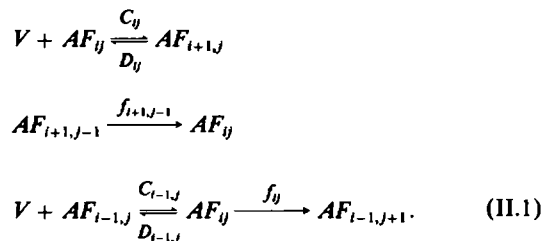
Finally, we have examined the kinetics of dimerization for two different particles. The aggregation and fusion of the mixed or asymmetric pair ($A + B \rightarrow AB \rightarrow$ fusion product) is described under the condition that neither of

Please address all correspondence to Dr. Joe Bentz.

the pure pairs ($A + A$ or $B + B$) can aggregate. These solutions will simplify the study of fusion between asymmetric vesicles, i.e., where the apposed membranes are quite different (Bentz et al., 1987; Stamatatos et al., 1988).

II. Mass Action Model and the General Kinetic Equations

In this section, we show the mass action reactions which govern virus-cell aggregation and fusion, as well as the kinetic equations which determine the evolution of the system over time. The molar concentration of cells with i virions adhering and j fused virions is denoted $[AF_{ij}]$. The following reactions determine the concentration of this species:



These reactions generate the following kinetic equations for the change in $[AF_{ij}]$ and the free virus concentration $[V]$ in time:

$$\begin{aligned} \frac{d[AF_{ij}]}{dt} = & -C_{ij}[V][AF_{ij}] + D_{ij}[AF_{i+1,j}] \\ & + f_{i+1,j-1}[AF_{i+1,j-1}] \\ & + C_{i-1,j}[V][AF_{i-1,j}] - (D_{i-1,j} + f_{ij})[AF_{ij}] \end{aligned} \quad (II.2)$$

$$\frac{d[V]}{dt} = \sum_{j=0}^{N_F-1} \sum_{i=0}^{N_B-1-j} \{-C_{ij}[V][AF_{ij}] + D_{ij}[AF_{i+1,j}]\}, \quad (II.3)$$

where N_F and N_B denote the total number of fusion sites and binding sites on the cell, respectively.

It has been found for Sendai virus that the maximum number of virus particles which can bind to an erythrocyte ghost exceeds the maximum number which can subsequently fuse with the ghost membrane (Nir et al., 1986b). It is not yet known whether the extent of fusion is limited by some threshold density of virial fusion proteins in the target membrane (due to fusion) which prohibits further fusion or whether only some of the binding sites are capable of supporting fusion. In any event, we will let N_F denote the maximum number of virions which can fuse with the cell. We assume that the fusion sites are a subset of the binding sites, i.e., the fusion event eliminates that binding site. It is obvious then that $[AF_{ij}] = 0$ if either $j > N_F$ or $i + j > N_B$. We note that if $N_B > N_F$, i.e., not all of the binding sites are fusion sites, then Eq. II.3 has the first summation (over j) from 0 to N_F , rather than $N_F - 1$.

We will first consider one simple model which assumes that the binding and fusion sites are identical and indepen-

dent. This implies that the rate at which free virus binds to the cell is strictly proportional to the number of remaining empty sites. Furthermore, the rate at which bound virus particles either fuse with or dissociate from the membrane is strictly proportional to the number of bound particles. Thus,

$$\begin{aligned} C_{ij} &= \frac{N_B - i - j}{N_B} C \\ D_{ij} &= (i + 1)D \\ f_{ij} &= if, \end{aligned} \quad (II.4)$$

where $C \equiv C_{00}$, $D \equiv D_{00}$, and $f \equiv f_{10}$, i.e., the rate constants for a cell with no competing bound or fused virus. In Section VI and Appendix D, we will treat the case of interacting binding sites, i.e., where they are not independent, under the condition that aggregation is rate limiting.

With this prescription of the rate constants, the kinetic equations are identical with those previously used by Nir et al. (1986b). The total concentration of cells, denoted G_0 , and of virus particles, denoted V_0 , satisfy the conservation relations

$$\begin{aligned} G_0 &= \sum_{j=0}^{N_F} \sum_{i=0}^{N_B-j} [AF_{ij}] \\ V_0 &= [V] + \sum_{j=0}^{N_F} \sum_{i=0}^{N_B-j} (i + j)[AF_{ij}]. \end{aligned} \quad (II.5)$$

Fig. 1 shows a sample calculation. Panel A gives the fraction of free cells, i.e., with no bound or fused virions ($[AF_{00}]/G_0$ in our notation), the fraction of free virus ($[V]/V_0$ in our notation), and the expected change in fluorescence intensity due to viral-cell fusion using a lipid

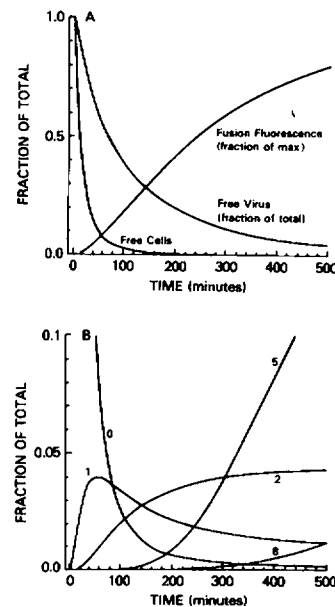


FIGURE 1 Exact values for the distribution of cells and virions during aggregation and fusion. For these calculations the following parameter values were used: $V_0 = 5 \times 10^{-13}$ M, $G_0 = 1 \times 10^{-13}$ M, $N_F = 10$, $C = 2 \times 10^9$ M⁻¹ s⁻¹, $f = 10^{-4}$ s⁻¹, and $D = 10^{-5}$ s⁻¹. The numerical solutions shown in Figs. 1-3 were obtained using the differential equation solver DGEAR (IMSL Library, Houston, Texas) which was run on a VAX 11/780 at the Laboratory of Mathematical Biology. The differential equation solver was imbedded in a general purpose simulation/plotting package written in VAX77 Fortran standard. Panel A shows the fraction of free cells, i.e., with no bound or fused virions ($[AF_{00}]/G_0$), free virus ($[V]/V_0$), and the fluorescence due to fusion, from Eqs. (II.2-4) and (III.1-3). Panel B shows the fraction of cells with only fused virions, and none bound, i.e., $[AF_{ij}]/G_0$, where the number of fused virions, j , is shown beside each curve.

mixing assay, as described in Section III. Panel B shows how some of the individual components of the cell distribution function behave. Here we have plotted the fraction of cells with j -fused virions and no other bound virions, i.e., $[AF_{0j}]/G_0$ in our notation, where the value of j is given beside each curve. What is obvious is that each species has its own time period of existence.

When there is no fusion, i.e., $f_{ij} = 0$ and the concentration $[AF_{ij}] = 0$ when $j > 0$, and the virus is binding to the identical and independent sites on the cell, then simple solutions for Eqs. (II.2 and 3) can be obtained (Perelson, 1985). Let $[A_i] = [AF_{i0}]$, since these are the only species with nonzero concentrations, and assume that there is no virus bound initially (i.e., $[V(t=0)] = V_0$). Then these solutions are,

$$\begin{aligned} \frac{[A_i]}{G_0} &= \binom{N_B}{i} T^i (1-T)^{N_B-i} \\ \frac{[V]}{V_0} &= \frac{[\bar{V}]}{V_0} + \frac{qP}{\exp\{q\tau\} - p}, \end{aligned} \quad (\text{II.6})$$

where,

$$\begin{aligned} T &= \frac{1 - [V]/V_0}{1 + \alpha} = \frac{V_0 - [V]}{NG_0} \\ \binom{N_B}{i} &= \frac{N_B!}{i!(N_B - i)!} \\ \frac{[\bar{V}]}{V_0} &= \frac{1}{2} \{q - (\alpha + K_D)\} \\ q &= [(\alpha + K_D)^2 + 4K_D]^{1/2} \\ p &= \frac{2 + \alpha + K_D - q}{2 + \alpha + K_D + q} \\ \tau &= \frac{CV_0 t}{N_B} \\ \alpha &= \frac{N_B G_0}{V_0} - 1 \\ K_D &= \frac{N_B D}{CV_0}. \end{aligned} \quad (\text{II.7})$$

T is the fraction of sites on the cell which are bound by virions and $[\bar{V}]$ is the equilibrium concentration of free virus.

It should be noted that the kinetics of virus binding here is precisely the same as if the sites were distributed homogeneously in the system (Tanford, 1961), i.e., the equivalent reaction is,



when S_0 = total molar concentration of cellular sites = $N_B G_0$ and $C' = C/N_B$. The rate of particle approach to each site is identical, whether it is on a cell surface or homoge-

neously distributed in the reaction volume. The scaling by the number of binding sites on the cell arises solely to transform C from the units of (molar concentration of cells) $^{-1}$ to C' in the units of (molar concentration of sites) $^{-1}$.

In Appendix D, we show that the general case of arbitrary higher order aggregation rate constants can be dramatically simplified when the aggregation is irreversible. This case subsumes that of irreversible aggregation rate-limiting fusion.

III. Fluorescence Assays for Fusion

Fluorometric assays can independently monitor the mixing of the membrane components and the encapsulated aqueous contents, and are uniquely suited to follow the rapid kinetics of virus-cell fusion because of their sensitivity. Here, we shall primarily consider lipid mixing assays (e.g., Struck et al., 1981; Hoekstra et al., 1984; Silvius et al., 1987), which have been used extensively in virus-cell and liposome-cell fusion studies (Citovsky et al., 1985; Stegmann et al., 1985, 1986, 1987a-c; Hoekstra et al., 1984, 1985; Hoekstra and Klappe, 1986; Nir et al., 1986a-c; Blumenthal et al., 1987; Stamatatos et al., 1988). Düzgüneş and Bentz (1988) have recently reviewed the fluorometric fusion assays and the methodology of their usage. Extension of our treatment to the more rigorous aqueous contents assays is straightforward.

The details of calibrating the fluorescence assays are given in Appendix C. We assume that the quantum efficiency of the fluorophore does not change due to virus-cell binding. Only dilution of the probes after fusion changes the fluorescence intensity, due to changes in Förster energy transfer. In this case, the important variable is the concentration of cells with j -fused virions, regardless of the number of bound virions. Thus, we define

$$F_j(t) = \sum_{i=0}^{N_B-j} [AF_{ij}]. \quad (\text{III.1})$$

The upper bound of the summation accounts for the fact that, for $F_j(t)$, j of the binding sites have fused.

If i_0 denotes the absolute fluorescence intensity initially (before fusion), i_t denotes the final absolute intensity (e.g., after membrane solubilization with detergent) and $i(t)$ denotes the absolute intensity at time t due to fusion, then the relative fluorescence intensity is

$$I(t) = \frac{i(t) - i_0}{i_t - i_0} = \frac{1}{V_0} \sum_{j=1}^{N_F} j B_j F_j(t), \quad (\text{III.2})$$

where B_j is the fluorescence per fluorophore after the fusion of j virions with the cell, relative to its maximal fluorescence.

The complete definition of B_j is given by Eq. (C.7). In the limit of infinite dilution of the probe into the cell membrane, $B_j = 1$ and $I(t)$ = the average number of fused virions per cell. Typically, $B_j < 1$ since there will be some

Förster energy transfer after fusion. The important parameter is $D_0 = \{\text{surface area of the cell } (S_G)/\text{surface area of the virus } (S_v)\}$. When $D_0 = S_G/S_v$ is large, then the quenching of the fluorophore in the cell membrane after fusion is a linear function of acceptor surface density and

$$B_j = \frac{1}{1 + j/D_0}. \quad (\text{III.3})$$

We will use this form for B_j in the subsequent calculations, because it conforms to the experimental configurations which we treat.

IV. Exact Solutions: Irreversible, Aggregation Rate-Limiting Fusion

In general, there is no closed form solution to the kinetic Eqs. (II.2) and (II.3), even with the simplifying assumptions on the structure of the higher order rate constants, Eq. (II.4). However, we will first consider the case of irreversible, aggregation rate-limiting fusion kinetics, where there is an exact solution. In Section V, we will use this solution to obtain accurate and simple approximate solutions for the general problem. For the remainder of this work, we will assume that all of the binding sites and the virions are fusogenic, i.e., $N_F = N_B$.

A. The Kinetics Equations. When the aggregation is irreversible ($D_{ij} = 0$) and the overall fusion reaction is rate limited by the aggregation step ($f_{ij} \gg C_{ij} [AF_{ij}]$), only the cell fusion products AF_{ij} have nonzero concentrations. Thus, we can simplify the notation by writing $[F_j] = [AF_{ij}]$. When there are no virions initially bound or fused, i.e., $[V(t=0)] = V_0$, we can solve Eq. (IV.2) immediately using the previously derived solution to the binding problem, Eq. (II.6), by setting $D = 0$. Thus,

$$\frac{[V]}{V_0} = \frac{\alpha}{(\alpha + 1) \exp \{\alpha \tau\} - 1}, \quad (\text{IV.1})$$

where $\alpha = (N_F G_0 / V_0) - 1$ and $\tau = CV_0 t / N_F$, as defined in Eq. (II.7) when $N_F = N_B$. It is useful to note that

$$\alpha \tau = \left(1 - \frac{V_0}{N_F G_0}\right) CG_0 t \quad (\text{IV.2})$$

so that in the limit of a large excess of cell fusion sites, i.e., $N_F G_0 \gg V_0$, we obtain (Nir et al., 1986b)

$$\frac{[V]}{V_0} \xrightarrow{N_F \rightarrow \infty} \exp \{-CG_0 t\}. \quad (\text{IV.3})$$

Now the solutions for the cell fusion products can be obtained using the solutions given by Perelson (1985), in that irreversible aggregation becomes irreversible aggregation-rate-limited fusion. Thus, from Eq. (II.6) with $N_B = N_F$ and $D = 0$,

$$\frac{[F_j]}{G_0} = \left(\frac{N_F}{j}\right) T^j (1 - T)^{N_F - j}, \quad (\text{IV.4})$$

where

$$T = \frac{1 - [V]/V_0}{\alpha + 1} = \frac{\exp \{\alpha \tau\} - 1}{(1 + \alpha) \exp \{\alpha \tau\} - 1} \xrightarrow{\alpha \rightarrow 0} = \frac{\tau}{1 + \tau}. \quad (\text{IV.5})$$

$T(\tau)$ is now the fraction of sites which have fused with a virion. Clearly, $T(0) = 0$ and

$$\lim_{\tau \rightarrow \infty} T = \begin{cases} \frac{1}{1 + \alpha} = \frac{V_0}{N_F G_0} & \alpha \geq 0 \\ 1 & \alpha \leq 0 \end{cases}. \quad (\text{IV.6})$$

B. Expected Fluorescence Intensities. From these solutions, we can develop a very simple analytical solution to the expected fluorescence intensity when the acceptor molecules are sufficiently dilute to use the linear dequenching function in Section III. We note first that under the assumption of aggregation-rate-limiting fusion, $F_j(t) = [F_j]$, see Eq. (III.1). Thus, Eqs. (III.2 and 3) and Eq. (IV.4) yield

$$I(t) = \frac{G_0}{V_0} \sum_{j=1}^{N_F} \left(\frac{N_F}{j}\right) T^j (1 - T)^{N_F - j} \frac{j}{1 + j/D_0}. \quad (\text{IV.7})$$

This equation is exact and not difficult to evaluate, provided that N_F is not too large. However, with some mild assumptions we can resolve it to a very simple closed form expression.

When the target membrane is large relative to the viral membrane, i.e., $D_0 = S_G/S_v \rightarrow \infty$, then we obtain

$$I(t) \xrightarrow{D_0 \rightarrow \infty} = \frac{G_0}{V_0} \sum_{j=1}^{N_F} \left(\frac{N_F}{j}\right) T^j (1 - T)^{N_F - j} = \frac{G_0}{V_0} N_F T \quad (\text{IV.8})$$

i.e., $I(t)$ simply equals the fraction of fused virus. We note that a fluorescence assay for contents mixing, corrected for any leakage during fusion, would usually follow Eq. (IV.8) (Düzgüneş and Bentz, 1988).

A more rigorous result for the case of finite dilution factors is derived in Appendix B using an asymptotic expansion of Eq. (IV.7). When $N_F \gg 1$ and $N_F/D_0 < 1$, then

$$I(t) \approx \frac{G_0}{V_0} \frac{N_F T}{1 + N_F T/D_0 + (D_0 + N_F T)^{-1}}. \quad (\text{IV.9})$$

This expression is extremely accurate, as will be shown in Table I below. The derivation of this expression is not simple, however we can illustrate its origin in the following way. It is easy to show that the average number of fused virions per cell is $\langle J \rangle = N_F T$, thus if all of the cells were fused to this average extent, then the relative fluorescence

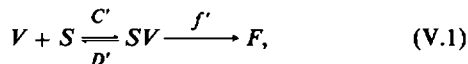
intensity from Eq. (III.2) would be

$$I_{\text{avg}} = \frac{G_0}{V_0} \frac{\langle J \rangle}{1 + \langle J \rangle / D_0} = \frac{G_0}{V_0} \frac{N_F T}{1 + N_F T / D_0}, \quad (\text{IV.10})$$

which is nearly the same as Eq. (IV.9). Eq. (IV.10) is also the expected fluorescence we would obtain by solving the homogeneous system $V + S \xrightarrow{C} F$, i.e., where the fusion sites are assumed to be homogeneously distributed in the system.

V. Approximate Solutions

We can now treat the general case where both aggregation reversibility and the fusion rate constant affect the overall fusion kinetics. In Section II, we saw that there was a close homology between the virus-cell adhesion problem and the case of homogeneously distributed binding sites. The same homology holds for the case of fusion. Here the homogeneous mass action reaction is



where S denotes the binding/fusion site and the primes on the rate constants mean that they refer to the homogeneous case. By our previous assumptions, we note that $C' = C/N_F$, $D' = D$ and $f' = f$, since both the fusion reaction and the dissociation step are properties of the binding/fusion site, per se. Here the initial concentration of sites $S_0 = [S(t=0)] = N_F G_0$. In Appendix A, we show that the kinetics of this reaction are adequately approximated by

$$\begin{aligned} \frac{[V]}{V_0} &= 1 - (\alpha + 1)T(\hat{\tau}) \\ \frac{[F]}{S_0} &= \mathcal{F}_1(\hat{K}, \hat{\tau})T(\hat{\tau}), \end{aligned} \quad (\text{V.2})$$

where

$$T(\hat{\tau}) = \frac{\exp\{\alpha\hat{\tau}\} - 1}{(1 + \alpha)\exp\{\alpha\hat{\tau}\} - 1} \quad (\text{V.3})$$

$\mathcal{F}_1 = 1 +$

$$\frac{\exp\{-\hat{K}\hat{\tau}\}[(\alpha\exp\{\alpha\hat{\tau}\})^2 - (\hat{K} - \alpha)(\exp\{\alpha\hat{\tau}\} - 1)^2] - \alpha^2\exp\{\alpha\hat{\tau}\}}{(\hat{K} - \alpha)(\exp\{\alpha\hat{\tau}\} - 1)((1 + \alpha)\exp\{\alpha\hat{\tau}\} - 1)} \quad (\text{V.4})$$

when $\alpha = 0$

$$\mathcal{F}_1 = 1 + \frac{\exp\{-\hat{K}\hat{\tau}\}[1 - \hat{K}\hat{\tau}^2] - 1}{\hat{K}\hat{\tau}(1 + \hat{\tau})}$$

or, when $\hat{K} = \alpha$,

$$\mathcal{F}_1 = 1 - \frac{\exp\{-\alpha\hat{\tau}\}[(\exp\{\alpha\hat{\tau}\} - 1)^2 + \hat{\tau}(\alpha\exp\{\alpha\hat{\tau}\})^2]}{(\exp\{\alpha\hat{\tau}\} - 1)((1 + \alpha)\exp\{\alpha\hat{\tau}\} - 1)}$$

and

$$\begin{aligned} \hat{\tau} &= \hat{C} V_0 t \\ \hat{K} &= \hat{f}/(\hat{C} V_0) \\ \hat{C} &= C'/(1 + D/f) = C/(N_F(1 + D/f)) \\ \hat{f} &= f(1 + D/f) \\ \alpha &= (S_0/V_0) - 1 = (N_F G_0/V_0) - 1. \end{aligned} \quad (\text{V.5})$$

\mathcal{F}_1 is a distribution function, i.e., $\mathcal{F}_1(\hat{K}, \hat{\tau}) \leq 1$, $\mathcal{F}_1(\hat{K}, 0) = 0$ and, $\mathcal{F}_1(\hat{K}, \infty) = 1$, which gives the fraction of the attached virus which has fused. When aggregation is rate limiting, \hat{K} is large (≥ 100) and $\mathcal{F}_1 \sim 1$. When fusion is rate limiting, \hat{K} is small (< 1) and $\mathcal{F}_1 \ll 1$.

Using the approach developed in Bentz et al. (1983, 1985), we will apply this result directly to the general system and approximate the expected relative fluorescence intensity from Eq. (IV.9) by

$$I(t) \approx \frac{G_0}{V_0} \frac{N_F T}{1 + N_F T/D_0 + (D_0 + N_F T)^{-1}} \mathcal{F}_1(\hat{K}, \hat{\tau}). \quad (\text{V.6})$$

Eq. (V.6) is a hybrid. The part excluding \mathcal{F}_1 is the (nearly) exact fluorescence intensity expected for virions fusing with cells under irreversible aggregation rate-limiting conditions. \mathcal{F}_1 is a good approximation for the fraction of attached virions which have in fact fused, for the homogeneous model. Simply multiplying the two functions

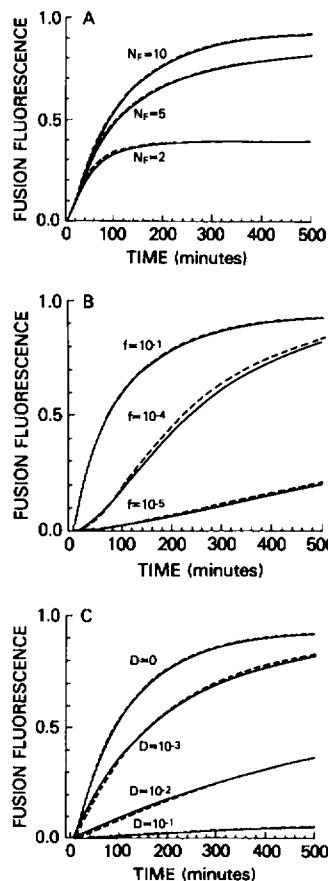


FIGURE 2 Comparison of approximate solution (dashed line, Eq. V.6) and the exact solution (solid line), for the fluorescence intensity due to virus-cell fusion. Unspecified parameters are the same as in Fig. 1. Panel A shows the effect of varying the number of binding sites per cell, $N_F = 2, 5$, and 10 , when $f = 10^{-3} \text{ s}^{-1}$ and $D = 0$. In these cases, $\hat{K} = 2-10$. Panel B shows the effect of varying the fusion rate constant, $f = 10^{-1}, 10^{-4}$, and 10^{-5} s^{-1} , when $D = 0$ and $N_F = 10$. In these cases, $\hat{K} = 10^{-1}$ to 10^{+3} . Panel C shows the effect of varying the dissociation rate constant, $D = 0, 10^{-3}, 10^{-2}$ and 10^{-1} s^{-1} , when $f = 10^{-3} \text{ s}^{-1}$ and $N_F = 10$. In these cases, $\hat{K} = 10$ to 10^{+5} .

together presumes that the homogeneous model gives a good estimate for the fraction of adhered virus which have fused for the cell model. The error in this premise is that it assumes that each species has the same fraction of fused-to-bound virions. In Fig. 1 *B*, we see how the fraction of fused virions for each species has its own time scale, which makes the assumption rigorously impossible. Nevertheless, the accuracy of the approximation, relative to the exact numerical integrations, shows that the average error (over the whole distribution) is typically negligible for the normal parameter ranges.

Fig. 2 shows the accuracy of Eq. (V.6) (dotted lines) relative to exact numerical integrations (solid lines) of the mass action equations. Panel A shows the effect of varying the number of fusion sites from 2 to 10. The approximate solution is quite good, even when $N_F = 2$. Panel B shows the effect of varying the fusion rate constant f , ranging from aggregation rate limiting, $f = 0.1 \text{ s}^{-1}$, where the approximate solution is nearly exact, to strongly fusion rate limiting ($f = 10^{-5} \text{ s}^{-1}$ and $\hat{K} = 0.1$), where the approximate solution is still in excellent agreement with the exact calculations. In these cases $D = 0$, so that $\hat{f} = f$ and $\hat{K} = K$. Finally, Panel C shows the effect of varying the dissociation rate constant D , ranging from irreversible aggregation to extremely reversible aggregation. A major factor in aligning the exact and approximate solutions is that increasing the value of D has the effect of making the fusion more aggregation rate limiting and improving the accuracy of the approximate solution.

It is clear from Fig. 2 that the approximation is quite accurate, even under adverse parameter values, such as strongly fusion rate-limiting kinetics (Fig. 2 *B*) or reversible aggregation (Fig. 2 *C*). We have found the combination of these two conditions will cause the approximate formula to deviate significantly from the exact solution, as shown in Fig. 3. The use of higher order approximations for \mathcal{F} (Eq. [A.11] in Appendix A) does not significantly improve the fit. On the other hand, if we treat the exact curves as data (with random error added), and fit them using Eq. (V.6), we obtain estimates for \hat{C} and \hat{f} which are not significantly different from the correct values

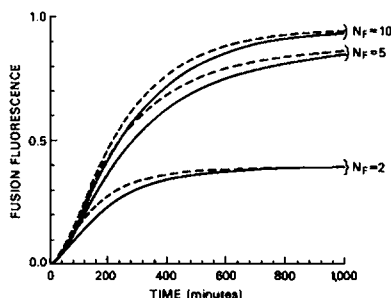


FIGURE 3 Comparison of approximate (dashed line) and exact (solid line) solutions when aggregation is reversible ($D/f = 0.1$) and the kinetics are strongly fusion rate limited ($\hat{K} = 0.242$ when $N_F = 2$ and $\hat{K} = 1.21$ when $N_F = 10$). Unspecified parameters are the same as in Fig. 1.

(C.V. = 30%). The quality of parameter estimates, however, will depend on the interval over which samples are taken as well as the sampling frequency.

Table I shows calculated and approximate values for the fluorescence intensity for large values of N_F . It is evident that the approximate solution is quite accurate when N_F is large. It must be noted that the usage of \mathcal{F}_1 as shown in Eq. (V.6) is a compromise between brevity and accuracy. For the parameters of the known virial fusion systems, this choice is adequate. For more extreme systems, the higher order approximations may be useful. However, when the aggregation kinetics are reversible and the overall reaction is rate limited by the fusion step, then accurate simulations cannot be obtained from Eq. (V.6).

DISCUSSION

The derivation of Eq. (V.6) for the fluorescence intensity due to virus-cell fusion has depended upon several assumptions. When aggregation is irreversible and rate limiting, i.e., $D/f \ll 1$ and $\hat{K} = N_F f / CV_0 \gg 1$, then the approximate

TABLE I
CALCULATED FLUORESCENCE INTENSITIES.
COMPARISON OF NUMERICAL INTEGRATION OF MASS
ACTION KINETIC EQUATIONS, EQS. (II.2-4), WITH THE
APPROXIMATE SOLUTION, EQ. (V.6)*

Case 1	t (min)	% Fluorescence Intensity, $I(t) \times 100$			
		$f(s^{-1}) = 0.01$		0.0001	
$N_F = 100$		Exact	Eq. (V.6)	Exact	Eq. (V.6)
$D(s^{-1}) = 0$	2	1.6	1.6	0.02	0.02
$D_0 = 500$	5	6.2	6.2	0.14	0.14
	10	14.1	14.2	0.5	0.53
	30	38.0	37.9	3.8	4.0
	60	58.8	58.8	11.8	12.4
Case 2		$D(s^{-1}) = 0.1$		0.2	
$N_F = 100$		Exact	Eq. (V.6)	Exact	Eq. (V.6)
$f(s^{-1}) = 0.08$	1	0.8	0.8	0.5	0.5
$D_0 = 500$	5	4.0	4.0	2.6	2.6
	15	11.5	11.5	7.7	7.7
	30	21.2	21.2	14.5	14.5
	45	29.4	29.4	20.6	20.6
Case 3		$D(s^{-1}) = 0$		0.005	
$N_F = 20$		Exact	Eq. (V.6)	Exact	Eq. (V.6)
$f(s^{-1}) = 0.001$	10	3.9	4.2	2.0	2.2
$D_0 = 100$	30	17.6	19.2	6.8	7.4
	60	31.0	32.5	12.5	13.5
	240	43.4	43.2	30.0	31.0
	360	43.8	43.6	35.0	35.7

*The following parameters were fixed: $C = 1.1 \times 10^9 \text{ M}^{-1} \text{ s}^{-1}$, $G_0 = 2.9 \times 10^{-13} \text{ M}$ and $V_0 = 1.1 \times 10^{-11} \text{ M}$. These values are typical for many experimental cases and provide wide ranges for the variables α , \hat{f} and \hat{K} . Eqs. (III.2 and 3) were used to calculate fluorescence intensities. For the approximate solution, Eq. (V.6) is used. Numerical integration of Eqs. (II.2 and 3) was performed using a Taylor series expansion, as explained in detail in Nir et al. (1986a, b).

equation is essentially exact since the only approximation is the extremely accurate closed form expression (Eq. [V.6] or [B.13]) for the exact summation, Eq. (IV.7). As the fusion step becomes rate limiting, i.e., $K \rightarrow 1$, then Eq. (V.6) becomes worse because we simply multiplied the expected fluorescence under aggregation rate-limiting kinetics, where all attached virus has fused, by the distribution function \mathcal{F}_1 , which is the fraction of attached virus which has fused for the homogeneous case. As the fusion step becomes rate limiting, the heterogeneity of the fused cell products becomes more apparent.

Actually, our derivation is based largely upon the assumption that there is little kinetic difference between having the binding/fusion sites on a cell surface and having them homogeneously distributed in the system. The validity of this assumption rests upon the structure of the higher order aggregation rate constants, C_{ij} . We have analyzed the case where the rate constant depended only upon the availability of binding sites, i.e., $C_{ij} = C(N_B - i - j)/N_B$, Eq. (II.4).

We can promptly treat one important corollary to this case which is when the number of fusion sites becomes (effectively) infinite. Liposome-virus fusion falls into this category because one virus fuses with any number of liposomes (Nir et al., 1986a,c). Here the liposomes assume the role of V and a fusion product of one virus and j liposomes is F_j . Under aggregation rate-limiting kinetics, see Eqs. (IV.5 and 10)

$$\begin{aligned} \frac{[V]}{V_0} &\xrightarrow{N_F \rightarrow \infty} \exp\{-CG_0 t\} \\ I_{avB} &\xrightarrow{N_F \rightarrow \infty} \frac{G_0}{V_0} \frac{\langle J \rangle}{1 + \langle J \rangle/D_0} \\ \langle J \rangle &\xrightarrow{N_F \rightarrow \infty} \frac{V_0}{G_0} (1 - \exp\{-CG_0 t\}). \end{aligned} \quad (VI.1)$$

For liposome-influenza virus fusion, $D_0 \sim 1$ (Nir et al., 1986a). These equations do not account for the possible aggregation of the virial fusion products.

In the other extreme, we can ask whether a more realistic accounting of surface binding will invalidate the usefulness of the homogeneous kinetic equations. Thakur et al. (1980) have considered the case of spheres attaching to a surface to discover how the random distribution occludes space using a gas phase model. The gist of their calculation is that an incoming sphere can reach the surface only if it does not collide with any portion of the already attached spheres. Given the angular dependence of trajectories near surfaces for gas phase kinetics, this substantially reduces the fraction of successful collisions. We believe that this model overestimates the occlusion of adjacent sites for particles undergoing Brownian motion, which can also execute diffusion along the cell surface (Berg and Purcell, 1977). Nevertheless, we shall see that even an overestimate of this magnitude does not seriously

compromise the approximate solution over the parameter values relevant to this problem.

When N spheres of cross-sectional area πa^2 are placed randomly on a surface of area S , then the fraction of occupied area is $p = N\pi a^2/S$ and the fraction of occluded area is approximately (Bell and Brown, 1974; Thakur et al., 1980)

$$f(p) = 1 - (1 - p) \exp\left\{-\frac{5p}{1-p}\right\}. \quad (VI.2)$$

If $p = 0.5$, i.e., half of the surface is covered, then, $f(p) = 0.997$, i.e., the model would predict that aggregation would proceed at vanishingly small rates, although at equilibrium there would still be full coverage. If the fusion sites are widely spaced, then this occlusion function is not important. However, if the entire cell surface is sticky, or the binding sites are closely packed, then higher order aggregation will be less rapid.

To estimate the magnitude of this correction, we will simply treat the case of irreversible binding, wherein the measurable property is the total amount of virus attached to the cells, whether fused or not. This case is identical to that of irreversible aggregation-rate-limited fusion. The worst case, with respect to the homogeneous solution, is when the entire surface is accessible to binding and the fraction of occupied area $p = i/N_B$, when i virions are bound. The fraction of remaining surface is $1 - f(p)$. Thus, we can introduce a shielding function g_i , which gives

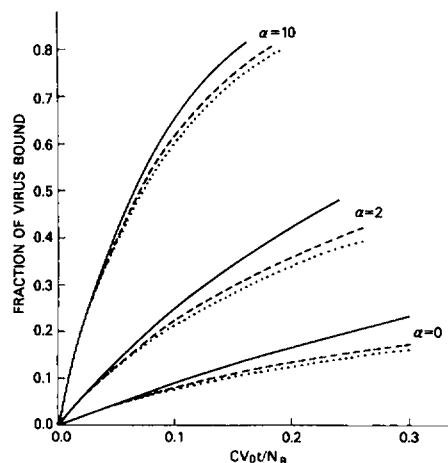


FIGURE 4 Fractions of virus bound as a function of shielding of adjacent sites by bound virus is calculated from Eqs. (D.9 and 10). Here only irreversible binding is being considered. The solid line indicates the binding when all binding sites are unshielded, i.e., identical and independent, where $g_i = 1$ in Eqs. (VI.3–4). The dashed line indicates the binding when the adjacent sites are shielded, where $g_i = \exp\{-5i/(N_B - 1)\}$ in Eq. (VI.4), and the number of sites per cell $N_B = 5$. The dotted line indicates the binding when the adjacent sites are shielded and $N_B > 20$, i.e. $N_B = 20$ or 50 gives the same values. The reduced time parameter $\tau = CV_0 t / N_B$ is used, where V_0 is fixed at $5 \times 10^{-13} M$, and the value of G_0 is altered to obtain the appropriate value of $\alpha = N_B V_0 / G_0 - 1$. Numerical integration of Eq. (D.10) was performed using a Romberg algorithm.

the reduction in C_{ij} , in excess of the loss of binding sites,

$$C_0 = C \left(\frac{N_B - i}{N_B} \right) g_i \quad (\text{VI.3})$$

$$g_i = \begin{cases} 1 & \text{when binding is unshielded} \\ \exp \left\{ -\frac{5i}{N_B - i} \right\} & \text{when binding is shielded.} \end{cases} \quad (\text{VI.4})$$

The values of C_{ij} for $j > 0$ are not relevant here. When the shielding function $g_i = 1$, then the results given in Section II are obtained. Fig. 4 shows the fraction of virus bound versus $\tau = CV_0t/N_B$ when binding is unshielded and when it is shielded. The virus concentration is fixed ($V_0 = 5 \times 10^{-13}\text{M}$) and the cell concentrations are varied such that $\alpha = 0, 2$, and 10 for each of the three cases. These values are calculated as described in Appendix D.

One general point is made. When binding is shielded, the error due to neglecting this event can be minimized by using excess binding sites, i.e., more cells, which is expected. One can neglect the existence of shielding until ~3–5% of the available area is covered.

It is interesting that the data fitted by Nir et al. (1986b) for Sendai virus fusing with erythrocyte ghosts differ from the theoretical curves, e.g., Eq. (V.6), in the same way as would be predicted if shielding of binding sites were occurring. Unfortunately, it is not yet possible to determine whether the shielding effect explains the data, since it is not known whether binding and fusion are over the entire erythrocyte membrane (where, due to the large area, shielding should be irrelevant) or over local patches of the membrane surface, where shielding could be quite important.

Once the virus has fused with the cell membrane, these strictly geometrical considerations would have no relevance to the aggregation rate constants. A detailed analysis of surface diffusion would be required (Berg and Purcell [1977]; Shoup et al. [1981]; Shoup and Szabo, 1982; Goldstein et al., 1988). An obvious consideration is whether all binding sites can fuse and whether fusion at one site affects adjacent sites.

Fitting the Rate Constants

The first step is determining N_F , the number of (virus) particles that can fuse with a single cell. This parameter is obtained from the final extents of fluorescence, i.e., from Eqs. (V.6) and (IV.6),

$$I(t) \xrightarrow{t \rightarrow \infty} \frac{G_0}{V_0} \frac{N_F}{1 + N_F/D_0 + (D_0 + N_F)^{-1}} \quad (\text{VI.5})$$

when $\alpha < 0$. The effective rate constants \hat{C} and \hat{f} can be fitted by performing the fusion experiment with several values of total virus concentration V_0 and cell concentrations G_0 , such that the ratio V_0/G_0 is constant. In this way, α is constant for all of the runs and as V_0 and G_0 become small, the overall fusion is rate limited by aggregation, i.e.,

$\mathcal{F}_1 = 1$ in Eq. (V.6). Once \hat{C} is determined under aggregation rate-limiting conditions, then \hat{f} can be fitted using the data for larger values of V_0 . If $D = 0$, then $\hat{C} = C'$ and $\hat{f} = f$. However, irreversible aggregation is not the general case.

An alternative way of fitting the rate constants, which has been used in practice, depends on the fact that the fluorescence curves predicted from Eq. (V.6) depend only upon \hat{C} at long times, where $\mathcal{F}_1(\hat{K}, \infty) = 1$. Thus, \hat{C} is obtained by looking at the later stages of the reaction. \hat{f} is obtained from fitting the initial stages. In practice, the virus concentration is kept constant and the cell concentration is varied. Of course, the use of a more concentrated cell suspension will enable a better determination of \hat{f} because fluorescence intensity values are larger in this case at the earlier times (Nir et al., 1986b).

Using the mass action kinetic model, the effective aggregation and fusion rate constants for several virus-cell and liposome-virus systems have been measured (Kuroda et al., 1985; Nir et al., 1986a–c; Tsao and Huang, 1986; Blumenthal et al., 1987). A discussion of the particular values of the rate constants, and the physical ramifications, can be found in Bentz and Ellens (1988). Overall, the values which we have used in Figs. 1–4 and Tables I and II are typical of the experimentally determined rate constants.

Reversibility and Preaggregation

The fact that the approximate solutions work so well using only the pair of reduced parameters $\hat{C} = C/(1 + D/f)$ and $\hat{f} = f(1 + D/f)$ means that rigorously fixing all three rate parameters C , D , and f will be difficult, if not impossible, using only the forward experiment. Determining the value of D/f requires a different experiment. The most useful approach appears to be binding the virions to the cells under nonfusogenic conditions (e.g., 4°C for Sendai virus and erythrocytes: Hoekstra and Klappe, 1986; Nir et al., 1986b) and then switch the condition to fusogenic, e.g., 37°C. The virions will either fuse or dissociate from the cell and both events can be independently monitored.

Since the dissociated virions will eventually attach to and fuse with other cells, the exact solution to this problem is not simple and requires extensive computer calculations. However, we can obtain an approximate answer, which is initially exact. We consider the homogeneous model given in Eq. (V.1) under the condition of preaggregation such that the concentration of bound virions is V_0 , there is no free virus, and all of the bound virus can either fuse with or dissociate from the cell membrane. Following the switch to the fusogenic conditions, the average number of fused virions per cell can be estimated by (Brendel and Perelson, 1987)

$$\langle J_p \rangle = \frac{V_0}{G_0} \frac{f}{D + f} (1 - \exp \{ -(D + f)t \}), \quad (\text{VI.6})$$

which is rigorously correct as long as the number of

dissociated virions which bind to new cells is negligible. In this time period, the free virus concentration is

$$\frac{[V]}{V_0} = \frac{D}{D+f} (1 - \exp \{-(D+f)t\}) \quad (\text{VI.7})$$

and the expected fluorescence due to fusion is, Eq. (IV.10),

$$I_{\text{avg}} = \frac{G_0}{V_0} \frac{\langle J_p \rangle}{1 + \langle J_p \rangle / D_0}. \quad (\text{VI.8})$$

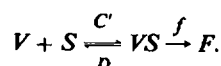
By measuring the fused virus concentration or the free virus concentration (or preferably both), it is possible to fix both f and D . While only the ratio D/f is required to determine C and f from \hat{C} and \hat{f} , the extra information gives two independent estimates for f .

In this regard, it is worth considering whether the preincubation experiment is sufficient if one is only interested in the fusion rate constant, as has been done by Kuroda et al. (1985), Nir et al. (1986b); Tsao and Huang (1986); and Blumenthal et al. (1987). Presently, there is no clear answer to this question. The studies cited have discussed various difficulties, as well as the controls proposed to account for their influence. We would add that the lengthy incubation time for binding should also increase the extent of multivalent interactions. This is likely to alter the cell surface, even before any fusion event is measured. Clearly, performing both types of experiment will provide far more reliable estimates of the rate constants. In a related issue, Richman et al. (1986) have emphasized that cells suffering multiple infections may show fusion mechanisms which differ from those found in vivo.

APPENDIX A

Kinetics of Heterogeneous Dimerization

We want to treat the reaction



Subject to the initial conditions $[V(t=0)] = V_0$ and $[S(t=0)] = S_0$ and the other species having zero concentration initially. The kinetic equations are

$$\begin{aligned} \frac{d[V]}{dt} &= \frac{d[S]}{dt} = -C'[V][S] + D[VS] \\ \frac{d[VS]}{dt} &= C'[V][S] - (f+D)[VS] \\ \frac{d[F]}{dt} &= f[VS]. \end{aligned} \quad (\text{A.1})$$

It is clear that $V_0 = [V] + [VS] + [F]$ at all times. Now, when we define the fraction of attached virions which have fused as

$$\mathcal{F} = \frac{[F]}{[F] + [VS]} \quad (\text{A.2})$$

then we can formally write

$$\begin{aligned} \frac{[VS]}{V_0} &= (1 - \mathcal{F}) \left(1 - \frac{[V]}{V_0} \right) \\ \frac{[F]}{V_0} &= \mathcal{F} \left(1 - \frac{[V]}{V_0} \right) \end{aligned} \quad (\text{A.3})$$

as well as the formal solution for $[F]/V_0$ as

$$\frac{[F]}{V_0} = \exp \{-ft\} \left[\frac{[F(0)]}{V_0} + f \int_0^t \exp \{fx\} \left(1 - \frac{[V(x)]}{V_0} \right) dx \right]. \quad (\text{A.4})$$

Therefore,

$$\mathcal{F} = \exp \{-ft\} \left[\frac{[F(0)]}{V_0} + f \int_0^t \exp \{fx\} \cdot \left(1 - \frac{[V(x)]}{V_0} \right) dx \right] \left/ \left(1 - \frac{[V(t)]}{V_0} \right) \right. \quad (\text{A.5})$$

This formal solution for \mathcal{F} is of value only if there is an explicit solution for $[V]$. Let us first consider the case of irreversible aggregation, i.e., $D = 0$. Then, we can use Eq. (IV.1) in the text to write

$$\begin{aligned} \frac{[V]}{V_0} &= 1 - (\alpha + 1)T(\tau) \\ T(\tau) &= \frac{\exp \{\alpha\tau\} - 1}{(1 + \alpha) \exp \{\alpha\tau\} - 1} \\ \alpha &= \frac{S_0}{V_0} - 1 \\ \tau &= C'V_0 t \\ K &= f/(C'V_0) \end{aligned} \quad (\text{A.6})$$

so that,

$$\frac{[F]}{V_0} = (\alpha + 1)T(\tau)\mathcal{F}(K, \tau). \quad (\text{A.7})$$

Thus, the solution for irreversible aggregation is at hand once the function \mathcal{F} is evaluated. This cannot be done in closed form, but there is an asymptotic solution. We write Eq. (A.5) in the dimensionless variables of Eq. (A.6), with $[F(0)] = 0$,

$$\begin{aligned} \mathcal{F} &= \frac{K}{T(\tau)} \int_0^\tau \exp \{-K(\tau - x)\} T(x) dx \\ &= \frac{K}{T(\tau)} \int_0^\tau \exp \{-Ks\} T(\tau - s) ds. \end{aligned} \quad (\text{A.8})$$

When $s = \tau - x$. Now let,

$$U(s) = \frac{\exp \{\alpha s\} - 1}{(1 + \alpha) \exp \{\alpha\tau\} - 1}. \quad (\text{A.9})$$

Then $U(s) < 1$ when $s < \tau$ and $U(\tau) = T(\tau)$. It can be shown that

$$\begin{aligned} T(\tau - s) &= \frac{T(\tau) - U(s)}{1 - U(s)} \\ &= T(\tau) + (T(\tau) - 1) \sum_{j=1}^{\infty} U(s)^j \end{aligned} \quad (\text{A.10})$$

and thus Eq. (A.8) becomes

$$\begin{aligned} \mathcal{F} &= K \int_0^\tau \exp\{-Ks\} ds \\ &+ K \frac{T(\tau) - 1}{T(\tau)} \sum_{j=1}^{\infty} \int_0^\tau \exp\{-Ks\} U(s)^j ds \\ &= 1 - \exp\{-K\tau\} - \frac{\exp\{\alpha\tau\}}{A} \sum_{j=1}^{\infty} \frac{W_j}{(A + \exp\{\alpha\tau\})^j}, \end{aligned} \quad (\text{A.11})$$

where

$$A = \frac{\exp\{\alpha\tau\} - 1}{\alpha} \xrightarrow{\alpha \rightarrow 0} \tau \quad (\text{A.12})$$

and

$$\begin{aligned} W_j &= \frac{K}{\alpha^j} \int_0^\tau \exp\{-Ks\} (\exp\{\alpha s\} - 1)^j ds \\ &= \frac{j! - \exp\{-K\tau\} \sum_{i=0}^j \frac{j!}{i!} \lambda_i A^i}{(\lambda_{j+1}/K)} \\ \lambda_j &= \prod_{i=0}^{j-1} (K - i\alpha). \end{aligned} \quad (\text{A.13})$$

Note that $\lambda_0 = 1$, $\lambda_1 = K$, $\lambda_2 = K(K - \alpha)$, $\lambda_3 = K(K - \alpha)(K - 2\alpha)$, and so on. Eq. (A.13) is well behaved in the event that $K \rightarrow i\alpha$, for any i , but the resulting equation is not as compact. Now,

$$W_1 = \frac{1 - \exp\{-K\tau\}(1 + KA)}{K - \alpha} \quad (\text{A.14})$$

and to first order

$$\mathcal{F}_1(K, \tau) = 1 - \exp\{-K\tau\} - \frac{\exp\{\alpha\tau\}}{A} \frac{W_1}{(A + \exp\{\alpha\tau\})}, \quad (\text{A.15})$$

when $\alpha = 0$

$$\mathcal{F}_1 = 1 - \exp\{-K\tau\} - \frac{1 - \exp\{-K\tau\}(1 + K\tau)}{K\tau(1 + \tau)},$$

when $K = \alpha$

$$\mathcal{F}_1 = 1 - \exp\{\alpha\tau\} - \frac{\alpha(1 + (\alpha\tau - 1)\exp\{\alpha\tau\})}{(\exp\{\alpha\tau\} - 1)((1 + \alpha)\exp\{\alpha\tau\} - 1)}.$$

Retaining the first two orders yields

$$\begin{aligned} \mathcal{F}_2(K, \tau) &= \mathcal{F}_1(K, \tau) \\ &+ \frac{\exp\{\alpha\tau\}}{A} \left[\frac{\exp\{-K\tau\}[K(K - \alpha)A^2 + 2KA + 2] - 2}{(K - \alpha)(K - 2\alpha)(A + \exp\{\alpha\tau\})^2} \right]. \end{aligned} \quad (\text{A.16})$$

If $\alpha = 0$, then $A = \tau$ and

$$\mathcal{F}_2 \xrightarrow{\alpha \rightarrow 0} \mathcal{F}_1 + \frac{1}{\tau} \left[\frac{\exp\{-K\tau\}[(K\tau + 1)^2 + 1] - 2}{K^2(1 + \tau)^2} \right]. \quad (\text{A.17})$$

In cases where $K = \alpha$ or $K = 2\alpha$, the appropriate limiting equations for \mathcal{F}_2 can be obtained easily. Typically, \mathcal{F}_3 is nearly exact.

The main problem with treating aggregation reversibility is that there is no analytical solution for $[V]/V_0$. However, in Bentz et al. (1983), it

TABLE II
FRACTION OF FUSED VIRUS, $[F]/V_0$. COMPARISON OF NUMERICAL INTEGRATIONS OF EQ. (A.2) WITH THE APPROXIMATE SOLUTION, EQ. (A.18)

$\frac{K}{\left(\frac{f}{C'V_0}\right)}$	D/f	τ ($C'V_0 t$)	$S_0/V_0 = 0.1$		$S_0/V_0 = 1.0$		$S_0/V_0 = 10.0$	
			Exact	Eq. (A.18)	Exact	Eq. (A.18)	Exact	Eq. (A.18)
100	0	0.05	0.0039	0.0039	0.038	0.038	0.322	0.322
		0.1	0.0086	0.0086	0.082	0.082	0.579	0.579
		0.5	0.038	0.038	0.329	0.329	0.989	0.989
		1.0	0.061	0.062	0.497	0.497	1.0	1.0
	2	0.01	0.0002	0.0002	0.0023	0.0023	0.022	0.022
		0.05	0.0016	0.0015	0.016	0.015	0.144	0.143
		0.1	0.0032	0.0032	0.031	0.031	0.267	0.272
		0.5	0.015	0.015	0.142	0.142	0.786	0.792
	0	0.1	0.0005	0.0005	0.0045	0.0046	0.035	0.035
		0.2	0.0017	0.0018	0.017	0.017	0.103	0.103
		1.0	0.026	0.029	0.218	0.230	0.589	0.589
		2.0	0.058	0.065	0.464	0.486	0.849	0.849
1	2	0.2	0.0015	0.0016	0.015	0.016	0.094	0.131
		1.0	0.017	0.020	0.151	0.181	0.521	0.811
		2.0	0.036	0.042	0.297	0.354	0.786	0.984
		10.0	0.091	0.095	0.727	0.763	1.0	1.0
	∞		0.1	0.1	1.0	1.0	1.0	1.0

Numerical integration of Eq. (A.2) was performed using a Runge-Kutta (order 4) algorithm.

was shown that the effect of reversibility could be approximated adequately using the equations from the irreversible case, provided that the rate constants were scaled. That is, the solution for the fused virus, $[F]$, can be estimated by

$$\frac{[F]}{V_0} \approx (\alpha + 1) \mathcal{F}_2(\hat{K}, \hat{\tau}) T(\hat{\tau}), \quad (\text{A.18})$$

where,

$$\begin{aligned} \hat{\tau} &= \hat{C} V_0 t \\ \hat{K} &= \hat{f} / (\hat{C} V_0) = K(1 + D/f)^2 \\ \hat{C} &= C' / (1 + D/f) \\ \hat{f} &= f(1 + D/f). \end{aligned}$$

Table II shows the accuracy of this equation relative to exact numerical integrations of Eq. (A.2) for a wide range of initial conditions. The approximation becomes inadequate for $\hat{K} < 1$ and $D/f > 2$. Using higher order terms for \mathcal{F} does not reduce the error of the approximation. It is interesting that this approach gives a much better approximation when used with the multisite virus-cell model, as is shown in Table I and Fig. 2. It is worth noting that \mathcal{F} is a weakly varying function of α , when $\alpha < 10$. This scaling of the rate constants gives a good approximation for the solution of the fused particles, $[F]/V_0$. In fact, Eq. (A.18) is asymptotically exact as $\tau \rightarrow 0$. The same approach will not give as good an approximation for the other species, which is to be expected since $[V]$ is initially independent of D (Bentz and Nir, 1981).

APPENDIX B

Resolution of the Fluorescence Intensity Function

Eq. (IV.7) shows that the fluorescence intensity expected for the lipid mixing assay is,

$$I(t) = \frac{G_0}{V_0} \sum_{j=1}^{N_F} \binom{N_F}{j} (1 - T)^{N_F-j} T^j \frac{j}{1 + j/D_0}. \quad (\text{B.1})$$

While this expression can be evaluated, we will find that a nontrivial expansion in powers of $1/D_0$ can be resolved into a very simple formula. The approximate formula is valid, and quite accurate, when $N_F/D_0 < 1$ and $N_F \gg 1$.

We begin by defining the function:

$$S_N(K, T) = \sum_{i=1}^N \binom{N}{i} i^K T^i (1 - T)^{N-i}. \quad (\text{B.2})$$

Expanding $(1 - T)^{N-i}$ gives

$$S_N(K, T) = \sum_{j=0}^{N-1} T^{N-j} \frac{N!}{j!} \sum_{i=1}^{N-j} (-1)^{N-i-j} \frac{i^K}{i!(N-i-j)!}. \quad (\text{B.3})$$

Now, if we take $\ell = N - j$, and define

$$\begin{aligned} a_{\ell K} &= \sum_{i=0}^{\ell} (-1)^{\ell-i} \frac{i^K}{i!(\ell-i)!} \\ b_{N\ell} &= \prod_{j=0}^{\ell-1} \left(1 - \frac{j}{N}\right) \end{aligned} \quad (\text{B.4})$$

so that $N!/(N - \ell)! = N^\ell b_{N\ell}$, then

$$S_N(K, T) = \sum_{\ell=1}^N (NT)^\ell b_{N\ell} a_{\ell K}. \quad (\text{B.5})$$

These $a_{\ell K}$ coefficients have interesting properties. It can be shown that

$$a_{\ell K} = 0 \quad \text{if} \quad \ell > K \geq 1 \quad (\text{B.6})$$

$$a_{KK} = a_{1K} = 1$$

$$a_{K,K+1} = K(K+1)/2$$

$$a_{K,K+2} = K(K+1)(K+2)(3K+1)/4!. \quad (\text{B.7})$$

Using Eq. (B.6), we can write Eq. (B.5) as

$$\begin{aligned} S_N(K, T) &= \sum_{\ell=1}^{\min(K,N)} (NT)^\ell b_{N\ell} a_{\ell K} \\ &= \sum_{i=\max(0, K-N)}^{K-1} (NT)^{K-i} b_{N,K-i} a_{K-i,K} \\ &\quad \text{with } i = K - \ell. \end{aligned} \quad (\text{B.8})$$

With these results, the resolution of Eq. (B.1) is straightforward. Noting that $1/(1+x) = \sum_{i=0}^{\infty} (-x)^i$ when $x < 1$, we can write

$$I(t) = \frac{G_0}{V_0} \sum_{i=0}^{\infty} (-D_0)^{-i} \sum_{j=1}^{N_F} \binom{N_F}{j} j^{i+1} T^j (1 - T)^{N_F-j}. \quad (\text{B.9})$$

Therefore, from Eq. (B.2) and (B.8)

$$\begin{aligned} I(t) &= \frac{G_0}{V_0} \sum_{i=0}^{\infty} (-D_0)^{-i} S_{N_F}(i+1, T) \\ &= \frac{G_0}{V_0} \sum_{i=0}^{\infty} (-D_0)^{-i} \sum_{j=\max(0, i-N_F)}^i (N_F T)^{i+1-j} b_{N_F, i+1-j} a_{i+1-j, i+1} \\ &= \frac{G_0}{V_0} \sum_{j=0}^{\infty} \sum_{i=j}^{N_F-1+j} (-D_0)^{-i} (N_F T)^{i+1-j} b_{N_F, i+1-j} a_{i+1-j, i+1} \\ &\quad \text{let } \ell = i - j \\ &= \frac{G_0}{V_0} N_F T \sum_{j=0}^{\infty} (-D_0)^{-j} \sum_{\ell=0}^{N_F-1} (-N_F T/D_0)^\ell b_{N_F, \ell+1} a_{\ell+1, \ell+1+j}. \end{aligned} \quad (\text{B.10})$$

Up to this point, our results are exact. Now, we will introduce two weak assumptions which will provide a simple closed from expression of $I(t)$. We assume that the number of fusion sites per cell is large, i.e., $N_F \gg 1$, and that the cell membrane is never increased in size by more than a factor of two due to the incorporation of virial membrane by fusion, i.e., $N_F/D_0 < 1$. With these assumptions, we can replace $b_{N_F, \ell}$ by 1, since Eq. (B.4) shows that this approximation is inaccurate only when $\ell \rightarrow N_F$, and then $(N_F T/D_0)^\ell \rightarrow 0$. We will also replace $N_F - 1$ by ∞ in the second summation, since the difference is numerically insignificant. Thus,

$$\begin{aligned} I(t) &\approx \frac{G_0}{V_0} N_F T \sum_{j=0}^{\infty} (-D_0)^{-j} \sum_{\ell=0}^{\infty} (-N_F T/D_0)^\ell a_{\ell+1, \ell+1+j} \\ &= \frac{G_0}{V_0} N_F T \sum_{j=0}^{\infty} Q_j (-D_0)^{-j}, \end{aligned} \quad (\text{B.11})$$

where,

$$Q_j = \sum_{\ell=0}^{\infty} (-N_F T/D_0)^\ell a_{\ell+1, \ell+1+j}.$$

Using Eq. (B.7), we find that $a_{t+1,t+1} = 1$, $a_{t+1,t+2} = (\ell+1)(\ell+2)/2$, and $a_{t+1,t+3} = (\ell+1)(\ell+2)(\ell+3)(3\ell+4)/4!$. Thus,

$$\begin{aligned} Q_0 &= \sum_{t=0}^{\infty} (-N_F T/D_0)^t = \frac{1}{1 + N_F T/D_0} \\ Q_1 &= \sum_{t=0}^{\infty} (-N_F T/D_0)^t \frac{(\ell+1)(\ell+2)}{2} \\ &= \frac{1}{(1 + N_F T/D_0)^2} \\ Q_2 &= \sum_{t=0}^{\infty} (-N_F T/D_0)^t \frac{(\ell+1)(\ell+2)(\ell+3)(3\ell+4)}{4!} \\ &= \frac{1 - N_F T/D_0}{(1 + N_F T/D_0)^3}. \end{aligned} \quad (\text{B.12})$$

We will make a further simplification. Following the pattern of Eq. (B.12), we can approximate $Q_j \approx (1 + N_F T/D_0)^{-(j+2)}$. Using this in Eq. (B.11) gives

$$I(t) \approx \frac{G_0}{V_0} \frac{N_F T}{1 + N_F T/D_0 + (D_0 + N_F T)^{-1}}. \quad (\text{B.13})$$

Eq. (B.13) is as accurate, or better, than Eq. (B.11) using terms up to Q_2 over the entire range of N_F and $D_0 > 1$, for those values of T where the relative error of both approximations is $< 1\%$. There is $< 1\%$ relative error for any value of N_F if $D_0 \geq 100$ and for $N_F \geq 50$ when $D_0 \geq 5$. Eq. (B.14) also has a simpler form than does the second order approximation of Eq. (B.11).

APPENDIX C

Fluorescence Assays for Membrane Fusion

As described in Düzgüneş and Bentz (1988), lipid mixing assays based upon resonance (or Förster) energy transfer depend upon the relative surface densities of the acceptor fluorophors, provided that the surface density of donors is not too great. Here, we shall develop the equations relevant to monitoring the fluorescence of the donor molecules and treat the dequenching configuration for the assay; wherein the donor and acceptor molecules are initially in one vesicle, i.e., the virus, and the fusion event results in a dequenching of the donor molecules as the probes are diluted into the target membrane.

Let q_0 denote the fluorescence intensity of the donor molecules in the absence of acceptor molecules, per unit molar concentration. Let n_d denote the number of donor molecules and n_a denote the number of acceptor molecules per virion. Let $q(v)$ equal the fraction of fluorescence quenching experienced by each donor molecule due to acceptor molecules in the same membrane at an effective density v = (surface density of acceptors) times R_0^2 , where R_0 is the distance for 50% energy transfer between the donor and acceptor molecules. Explicit equations for $q(v)$ can be found in Wolber and Hudson (1979); Snyder and Friere (1982); and Düzgüneş and Bentz (1988). In general, $q(v) < 1$, $q(0) = 1$ and $q(\infty) = 0$. The initial fluorescence intensity is

$$i_0 = V_0 n_d q(n_a R_0^2/S_v) q_0, \quad (\text{C.1})$$

where S_v is the surface of the virus. The final fluorescence intensity will depend upon the surface area of the cell membrane relative to the viral membrane area. If S_G denotes the surface area per cell and all the virions can fuse with the cell, then $D_f = (V_0 S_v + G_0 S_G)/(V_0 S_v)$ is the final (average) dilution factor for the acceptor molecules. Therefore, the final fluorescence intensity is

$$i_f = V_0 n_d q(n_a R_0^2/D_f S_v) q_0, \quad (\text{C.2})$$

where we have neglected the possible, and correctable, problem of extraneous energy transfer to, or from, cell membrane components (Stamatatos et al., 1988).

In order to obtain the change in fluorescence intensity due to fusion, we need to sum the concentrations of cells which have the same number of fused virus, regardless of the number of bound virus, as we assumed that simple binding has no effect on the fluorescence of the donor molecules. We define

$$F_j(t) = \sum_{i=0}^{N_F-j} [AF_{ij}]. \quad (\text{C.3})$$

Thus, $F_j(t)$ is the molar concentration of cells with j fused virions. The upper bound of the summation accounts for the fact that j of the binding sites have been fused.

It will be notationally convenient to define

$$D_j = (S_G + jS_v)/S_v = j + D_0, \quad (\text{C.4})$$

where $D_0 = S_G/S_v$ is the relative surface area of the cell to that of the virus. After fusion, the absolute fluorescence intensity is

$$\begin{aligned} i(t) &= \left(V_0 - \sum_{j=1}^{N_F} jF_j(t) \right) n_d q(n_a R_0^2/S_v) q_0 \\ &\quad + \sum_{j=1}^{N_F} jF_j(t) n_d q(jn_a R_0^2/D_j S_v) q_0. \end{aligned} \quad (\text{C.5})$$

Therefore, the relative change in fluorescence is:

$$I(t) = \frac{i(t) - i_0}{i_f - i_0} = \frac{1}{V_0} \sum_{j=1}^{N_F} jB_j F_j(t) \quad (\text{C.6})$$

$$B_j = \frac{q(jn_a R_0^2/D_j S_v) - q(n_a R_0^2/S_v)}{q(n_a R_0^2/D_f S_v) - q(n_a R_0^2/S_v)}. \quad (\text{C.7})$$

Notice that the function $I(t)$ is defined such that $I(0) = 0$, $I(t)$ increases in time due to fusion and $I(t) = 1$, only if all of the virions have fused.

We will specifically consider the case where the surface density of acceptor molecules in the target membrane after fusion is sufficiently small that the quenching function $q(v)$ is linear with respect to v , which requires < 1 acceptor per $5R_0^2$ (Wolber and Hudson, 1979; Snyder and Friere, 1982; Düzgüneş and Bentz, 1988). For most lipid mixing assays, this condition is met when the acceptor is present at ≤ 0.5 mol % lipid in the cell membrane (Struck et al., 1981; Hoekstra et al., 1984; Silvius et al., 1987).

In this case, we can write

$$B_j = \frac{1}{1 + j/D_0} \cdot \left(\frac{1}{1 - 1/D_f} \right). \quad (\text{C.8})$$

Another step is usually introduced for experimental convenience: the final signal i_f is set by lysing the virus-cell suspension in detergent. This simplifies setting the value for i_f , although it is an artificial state and care must be taken to assure that no artifactual quenching of the fluorophors occurs due to the presence of the detergent (Tanaka and Schroit, 1983). We can treat this as a case of infinite dilution ($D_f = \infty$) and Eq. (C.6) becomes

$$I(t) = \frac{1}{V_0} \sum_{j=1}^{N_F} F_j(t) \frac{j}{1 + j/D_0}. \quad (\text{C.9})$$

It is worthwhile recalling that $\sum_{j=1}^{N_F} jF_j(t)/V_0$ is just the fraction of virus which has fused. Thus, when $D_0 \rightarrow \infty$, i.e., the cell membrane is vastly larger than the viral membrane and fusion implies an infinite dilution of probe, then $I(t)$ exactly equals the fraction of virus which has fused. In general, $I(t)$ will be less than this fraction.

APPENDIX D

The General Solution for Irreversible Aggregation

Here we show that the general adhesion model



can be completely determined by the integration of a single ordinary differential equation. This case covers irreversible aggregation, Section II, and irreversible aggregation rate limited fusion, Section IV, where F_i would replace A_i . We will write

$$C_i = C \left(\frac{N-i}{N} \right) g_i \quad (D.2)$$

so that g_i is the shielding function for adjacent binding sites, as defined in Eq. (VI.4). However, we will not specify g_i any further; which makes the values of C_i arbitrary. N is just the total number of binding sites (in which case, $N = N_B$) or the total number of fusion sites (in which case, $N = N_F$).

When we define $\tau = C_0 V_0 t / N$, $\nu = [V] / V_0$ and $x_i = [A_i] / V_0$, then the mass action equations for Eq. (D.1) are

$$\begin{aligned} \frac{d\nu}{d\tau} &= -\nu \sum_{i=0}^{N-1} (N-i) g_i x_i \\ \frac{dx_i}{d\tau} &= \nu \{ (N+1-i) g_{i-1} x_{i-1} - (N-i) g_i x_i \}. \end{aligned} \quad (D.3)$$

Let us now define,

$$z(\tau) = \int_0^\tau \nu(u) du \quad (D.4)$$

and write Eq. (D.3) in terms of z . Thus,

$$\frac{d\nu}{dz} = -\sum_{i=0}^{N-1} (N-i) g_i x_i \quad (D.5)$$

$$\frac{dx_i}{dz} = (N+1-i) g_{i-1} x_{i-1} - (N-i) g_i x_i. \quad (D.6)$$

Now Eq. (D.6) has a formal solution with respect to z for all i , which is

$$x_i = \exp \{ -(N-i) g_i z \} \int_0^z \exp \{ (N-i) g_i u \} \cdot [(N+1-i) g_{i-1} x_{i-1}(u)] du$$

which can be solved inductively to yield

$$x_i = \frac{G_0}{V_0} \sum_{j=0}^i \beta_{ij} \exp \{ -(N-j) g_j z \} \quad (D.7)$$

by noting that $dx_0/d\tau = -N g_0 x_0$, $g_0 = 1$ and $x_0(0) = G_0/V_0$. Here

$$\begin{aligned} \beta_{ij} &= -\beta_{i-1,j} \frac{(N+1-i) g_{i-1}}{(N-j) g_j - (N-i) g_i} \quad j < i \\ \beta_{ii} &= -\sum_{j=0}^{i-1} \beta_{ij} \\ \beta_{00} &= 1. \end{aligned} \quad (D.8)$$

Given these solutions for x_i , we can integrate Eq. (D.5) immediately and obtain

$$\begin{aligned} \nu &= \frac{[V]}{V_0} = 1 - (1 + \alpha) \sum_{i=0}^{N-1} \gamma_i [1 - \exp \{ -(N-i) g_i z \}] \\ \gamma_i &= [N(N-i) g_i]^{-1} \sum_{j=i}^{N-1} (N-j) g_j \beta_{ji}. \end{aligned} \quad (D.9)$$

This gives the solution for ν and x_i in terms of z . Now, from the definition of z , Eq. (D.4) we can write

$$\begin{aligned} \tau &= \int_0^z \frac{du}{[V(u)]/V_0} \\ &= \int_0^z \frac{du}{1 - (1 + \alpha) \sum_{i=0}^{N-1} \gamma_i [1 - \exp \{ -(N-i) g_i u \}]}, \end{aligned} \quad (D.10)$$

which is an ordinary integral giving τ as a function of z . The easiest approach is to choose z and evaluate τ .

In the case of fusion, which is rate limited by irreversible aggregation, we can immediately write the equation for the expected fluorescence intensity as

$$\begin{aligned} I(t) &= \frac{G_0}{V_0} \sum_{i=0}^{N_F} \xi_i \exp \{ -(N-i) g_i z \} \\ \xi_i &= \sum_{j=i}^{N_F} \frac{j}{1 + j/D_0} \beta_{ji} \end{aligned} \quad (D.11)$$

using Eqs. (III.1-3) and (D.7), since under these conditions, x_i is identical to $F_i(t)/V_0$.

We note that if the binding sites are independent, then $g_i = 1$ and

$$\begin{aligned} \beta_{ij} &= (-1)^{i+j} \binom{N}{i} \binom{i}{j} \\ \gamma_i &= \begin{cases} 0 & \text{if } i < N-1 \\ 1 & \text{if } i = N-1 \end{cases} \\ z &= \ln \left[\frac{(\alpha+1) \exp \{ \alpha \tau \} - 1}{\alpha \exp \{ \alpha \tau \}} \right] \xrightarrow{\alpha \rightarrow 0} \ln \{ 1 + \tau \}. \end{aligned} \quad (D.12)$$

Eqs. (D.9 and D.11) now reduce to Eqs. (II.6 and IV.7), respectively.

These nearly closed form solutions reduce the number of differential equations to be numerically integrated from N to 1. When aggregation is reversible, it appears that the entire ensemble of equations must be numerically integrated to obtain the exact solutions. Nevertheless, it should be possible to develop approximate analytical solutions using the equations for irreversible aggregation presented here and the approach of scaling parameters presented here and previously (Bentz and Nir, 1981; Bentz et al., 1983).

We wish to thank Andrea Mazel for the expert and patient typing of this manuscript.

This investigation was supported by research grant GM-31506 (Joe Bentz and Shlomo Nir) from the National Institutes of Health and partially supported by the United States-Israel Binational Science Foundation (BSF) grant 86-00010 (Shlomo Nir).

Received for publication 3 February 1988 and in final form 13 May 1988.

REFERENCES

- Bell, W. K. and L. F. Brown. 1974. Kinetic theory approach to simultaneous gas and surface diffusion in capillaries. *J. Chem. Phys.* 61:609-618.
- Bentz, J., and H. Ellens. 1988. Membrane fusion: kinetics and mechanisms. *Colloids Surf.* 30:65-112.
- Bentz, J., and S. Nir. 1981. Mass action kinetics and equilibria of reversible aggregation. *J. Chem. Soc. Faraday Trans. I.* 77:1249-1275.
- Bentz, J., S. Nir, and J. Wilschut. 1983. Mass action kinetics of vesicle aggregation and fusion. *Colloids Surf.* 6:333-363.
- Bentz, J., N. Düzgüneş, and S. Nir. 1985. Temperature dependence of divalent cation induced fusion of phosphatidylserine liposomes: evaluation of the kinetic rate constants. *Biochemistry.* 24:1064-1072.
- Bentz, J., H. Ellens, and F. C. Szoka. 1987. Destabilization of phosphatidylethanolamine containing liposomes: hexagonal phase and asymmetric membranes. *Biochemistry.* 26:2105-2116.
- Bentz, J., D. Alford, J. Cohen, and N. Düzgüneş. 1988. La^{3+} -induced fusion of phosphatidylserine liposomes. Close approach, intermembrane intermediates, and the electrostatic surface potential. *Biophys. J.* 53:593-607.
- Berg, H. C., and E. M. Purcell. 1977. Physics of chemoreception. *Biophys. J.* 20:193-219.
- Blumenthal, R. 1987. Membrane Fusion. *Curr. Top. Membr. Transp.* 29:203-254.
- Blumenthal, R., A. Bali-Puri, A. Walter, D. Covell, and O. Eidelman. 1987. pH-Dependent fusion of Vesicular Stomatitis virus with Vero cells: measurement by dequenching of octadecyl rhodamine fluorescence. *J. Biol. Chem.* 262:13614-13619.
- Brendel, V., and A. S. Perelson. 1987. Kinetic analysis of adsorption processes. *SIAM (Soc. Ind. Appl. Math.) J.* 47:1306-1319.
- Citovsky, V., R. Blumenthal, and A. Loyter. 1985. Fusion of Sendai virions with phosphatidylcholine-cholesterol liposomes reflects the viral activity required for fusion with biological membranes. *FEBS (Fed. Eur. Biochem. Soc.) Lett.* 193:135-140.
- Doxsey, S., J. Sambrook, A. Helenius, and J. White. 1985. An efficient method for introducing macromolecules into cells. *J. Cell Biol.* 101:19-27.
- Düzgüneş, N., and J. Bentz. 1988. Fluorescence assays for membrane fusion. In *Spectroscopic Membrane Probes*. L.M. Loew, editor. CRC Press Inc., Boca Raton, FL. Vol. 1 117-159.
- Gani, J. 1965. Stochastic phage attachment to bacteria. *Biometrics.* 21:134-139.
- Gani, J. 1967. A problem of virus populations: attachment and detachment of antibodies. *Math. Biosci.* 1:545-554.
- Goldstein, B., C. Wofsy, and H. Echavarría-Heras. 1988. Effect of membrane flow on the capture of receptors by coated pits. *Biophys. J.* 53:405-414.
- Hoekstra, D., and K. Klappe. 1986. Sendai virus-erythrocyte membrane interaction: quantitative and kinetic analysis of viral binding, dissociation, and fusion. *J. Virol.* 58:87-95.
- Hoekstra, D., T. de Boer, K. Klappe, and J. Wilschut. 1984. Fluorescence method for measuring the kinetics of fusion between biological membranes. *Biochemistry.* 23:5675-5681.
- Hoekstra, D., K. Klappe, T. de Boer, and J. Wilschut. 1985. Characterization of the fusogenic properties of Sendai virus: kinetics of fusion with erythrocyte membranes. *Biochemistry.* 24:4739-4745.
- Kuroda, K., K. Kawasaki, and S. Ohnishi. 1985. Kinetic analysis of fusion of hemagglutinating virus of Japan with erythrocyte membranes using spin-labeled phosphatidylcholine. *Biochemistry.* 24:2624-2629.
- Nir, S., T. Stegmann, and J. Wilschut. 1986a. Fusion of influenza virus and cardiolipin liposomes at low pH: mass action analysis of kinetics and extent. *Biochemistry.* 25:257-266.
- Nir, S., K. Klappe, and D. Hoekstra. 1986b. Kinetics and extent of fusion between Sendai virus and erythrocyte ghosts: application of a mass action kinetic model. *Biochemistry.* 25:2155-2161.
- Nir, S., K. Klappe, and D. Hoekstra. 1986c. Mass action analysis of kinetics and extent of fusion between Sendai virus and phospholipid vesicles. *Biochemistry.* 25:8261-8266.
- Perelson, A. S. 1985. A model for antibody mediated cell aggregation: Rosette formation. In *Mathematics and Computers in Biomedical Applications*. J. Eisenfeld and C. DeLisi, editors. Elsevier Science Publishers, North Holland, N.Y. 31-37.
- Redmond, S., G. Peters, and C. Dickson. 1984. Mouse mammary tumor virus can mediate cell fusion at low pH. *Urology.* 133:393-402.
- Richman, D. D., K. Y. Hostetler, P. J. Yazaki, and S. Clark. 1986. Fate of influenza A virion proteins after entry into subcellular fractions of LLC cells and the effect of amantadine. *Virology.* 151:200-210.
- Shoup, D., G. Lipari, and A. Szabo. 1981. Diffusion controlled biomolecular reaction rates. The effect of rotational diffusion and orientation constraints. *Biophys. J.* 36:697-714.
- Shoup, D., and A. Szabo. 1982. Role of diffusion in ligand binding to macromolecules and cell-bound receptors. *Biophys. J.* 40:33-39.
- Silvius, J. R., R. Leventis, P. M. Brown, and M. Zuckermann. 1987. Novel fluorescent phospholipids for assays of lipid mixing between membranes. *Biochemistry.* 26:4279-4287.
- Snyder, B., and E. Friere. 1982. Fluorescence energy transfer in two dimensions: a numeric solution for random and nonrandom distributions. *Biophys. J.* 40:137-148.
- Stamatatos, L., R. Leventis, M. Zuckermann, and J. R. Silvius. 1988. Interactions of cationic lipid vesicles with negatively charged phospholipid vesicles and biological membranes. *Biochemistry.* 27:3917-3925.
- Stegmann, T., D. Hoekstra, G. Scherphof, and J. Wilschut. 1985. Kinetics of pH-dependent fusion between Influenza virus and liposomes. *Biochemistry.* 24:3107-3113.
- Stegmann, T., D. Hoekstra, G. Scherphof, and J. Wilschut. 1986. Fusion activity of Influenza virus: a comparison between biological and artificial target membrane vesicles. *J. Biol. Chem.* 261:10966-10969.
- Stegmann, T., F. Booy, and J. Wilschut. 1987a. Effect of low pH on influenza virus: Activation and inactivation of the membrane fusion capacity of the hemagglutinin. *J. Biol. Chem.* 262:17744-17749.
- Stegmann, T., H. W. M. Morselt, J. Scholma, and J. Wilschut. 1987b. Direct measurement of the fusion of influenza virus in an intracellular acidic compartment. *Biochim. Biophys. Acta.* 904:165-170.
- Stegmann, T., H. W. M. Morselt, F. P. Booy, J. F. L. van Breeman, G. Scherphof, and J. Wilschut. 1987c. Functional reconstitution of influenza virus envelopes. *EMBO (Eur. Mol. Biol. Organ.) J.* 6:2651-2659.
- Struck, D. K., D. Hoekstra, and R. E. Pagano. 1981. Use of resonance energy transfer to monitor membrane fusion. *Biochemistry.* 20:4093-4099.
- Tanaka, Y., and A. Schroit. 1983. Insertion of fluorescent phosphatidylserine into the plasma membrane of red blood cells. *J. Biol. Chem.* 258:11335-11343.
- Tanford, C. 1961. *Physical Chemistry of Macromolecules*. John Wiley & Sons, Inc., New York. 261-263.
- Thakur, S. C., L. F. Brown, and G. F. Haller. 1980. Gas-adsorbate collisional effects and surface diffusion in porous materials. *A.I.Ch.E.J.* 26:355-363.
- Tsao, Y.-S., and L. Huang. 1986. Kinetic studies of Sendai virus-target membrane interactions. Independent analysis of binding and fusion. *Biochemistry.* 25:3971-3976.
- van Meer, G., J. Davoust, and K. Simons. 1985. Parameters affecting low-pH-mediated fusion of liposomes with the plasma membrane of cells infected with Influenza virus. *Biochemistry.* 24:3593-3602.
- White, J., M. Kielian, and A. Helenius. 1983. Membrane fusion proteins of enveloped animal viruses. *Q. Rev. Biophys.* 16:151-195.
- Wolber, P. K., and B. S. Hudson. 1979. An analytic solution to the Förster energy transfer problem in two dimensions. *Biophys. J.* 28:197-210.
- Yassky, D. 1962. A model for the kinetics of phage attachment to bacteria in suspension. *Biometrics.* 18:185-191.